Iranian Journal of Oil & Gas Science and Technology, Vol. 4 (2015), No. 2, pp. 27-39
http://ijogst.put.ac.ir

An Improvement in Temporal Resolution of Seismic Data Using Logarithmic Time-frequency Transform Method

Amin Roshandel Kahoo[*] and Saman Gholtashi

[1] School of Mining, Petroleum and Geophysics Engineering, University of Shahrood, Shahrood, Iran

Received: December 05, 2014*; revised:* February 18, 2015*; accepted:* March 14, 2015

Abstract

The improvement in the temporal resolution of seismic data is a critical issue in hydrocarbon exploration. It is important for obtaining more detailed structural and stratigraphic information. Many methods have been introduced to improve the vertical resolution of reflection seismic data. Each method has advantages and disadvantages which are due to the assumptions and theories governing their issues. In this paper, we improve the temporal resolution of reflection seismic data using the logarithmic time-frequency transform method. This method has minimum user-defined parameters. The algorithm uses valuable properties of both the time-frequency transform and the cepstrum to extend the frequency band at each translation of the spectral decomposing window. In this method, the displacement of amplitude spectrum by its logarithm is the basic idea of the algorithm. We tested the mentioned algorithm on both synthetic and real data. The results of the both tests show that the introduced method can increase the temporal resolution of seismic data.

Keywords: Seismic Temporal Resolution, Time-frequency Transform, Logarithmic Method, Enhancing Temporal Resolution

1. Introduction

There are two types of resolutions in surface reflection seismic data, namely horizontal resolution and vertical resolution. The vertical or temporal resolution is expressed by the tuning thickness and the horizontal or spatial resolution is expressed by the Fresnel zone (Badley, 1985). The improvement in the temporal resolution of seismic data is a critical subject in hydrocarbon exploration and characterizing thin-layered hydrocarbon reservoirs. It is used for obtaining more detailed structural and stratigraphic information.

Tuning thickness is defined as a quarter of the dominant wavelength at the position of the target layer (Sheriff and Geldart, 1995). The tuning thickness is related to the interval velocity of target layer and dominant frequency of the traveling wave at the depth of the target layer. Therefore, the increase in the dominant frequency of seismic data can help to improve the temporal resolution.

Many methods have been introduced to increase the vertical resolution of reflection seismic data. Inverse Q-filter (Wang, 2008), different deconvolution methods (Yilmaz and Doherty, 2001) and time-variant spectral whitening (Yilmaz and Doherty, 2001) are the basic methods of the resolution

[*] Corresponding Author:
Email: roshandel@shahroodut.ac.ir

improvement. In the deconvolution procedure, the band limited seismic source signature is compressed by various methods to increase the frequency band of seismic source wavelet.

The wavelet transform and time-frequency representation are the basis of many methods of vertical resolution improvement to seismic data (Matos and Marfurt, 2014; Sajid and Ghosh, 2014; Shang and Caldwell, 2003; Zhou et al., 2014). Shang and Caldwell (2003) improved the bandwidth of seismic data based on high-order cumulant wavelet analysis. Matos and Marfurt (2014) broadened the seismic trace spectrum by creating a high resolution seismic trace guided by the complex continuous wavelet transform ridges detected along the scales. Zhou et al. (2014) proposed an improved time-frequency spectral modeling deconvolution method to enhance the seismic temporal resolution.

Cepstrum analysis is one of the mathematical tools frequently used in seismic data processing. Herra and van der Baan (2012) applied the cepstrum theory to estimate the seismic wavelet. In this paper, the cepstrum theory (Oppenheim et al., 1997) was used to improve the temporal resolution of reflection seismic data. The inverse Fourier transform of the logarithm of the amplitude spectrum of a signal is named the cepstrum (Sajid and Ghosh, 2014). Herein, the cepstrum was extended to time-frequency representation. The mentioned algorithm is applied to synthetic and real seismic data.

2. Methodology

First, the method of resolution improving based on cepstrum in Fourier domain is introduced. This method consists of three steps. In the first step, the time domain signal, $x(t)$, is transformed to frequency domain (f) by Fourier transform formula (Proakis and Manolakis, 2007) as given in Equation 1. Then, the amplitude and phase spectrum are calculated from the Fourier transform of signal as denoted in Equation 2.

$$X(f) = \int_{-\infty}^{+\infty} x(t) e^{-j\omega t} dt \tag{1}$$

$$\begin{aligned} &\text{Amplitude Spectrum} = A(f) = |X(f)| \\ &\text{Phase Spectrum} = \Phi(f) = \measuredangle X(f) \end{aligned} \tag{2}$$

where, $x(t)$ is the time domain signal, $X(f)$ is the Fourier transform of the time domain signal, and $A(f)$ and $\Phi(f)$ are the amplitude and phase spectrum of time domain signal respectively. In the next step, the amplitude spectrum of the signal is extended by replacing it with its logarithm. The phase spectrum of the signal remains unchanged in this procedure.

In the third step, the minimum value of the logarithmic amplitude spectrum subtracted from all spectral values to make the logarithmic amplitude spectrum positive. In order to make the total energy of logarithmic amplitude spectrum equal before and after the whitening, the logarithmic amplitude spectrum is normalized by its total energy (Sajid and Ghosh, 2014). The high resolution seismic trace can be reconstructed by using the normalized logarithmic amplitude spectrum and the unchanged phase spectrum.

The mentioned algorithm was tested on a 15 Hz Ricker wavelet (Sheriff and Geldart, 1995) and the results are shown in Figure 1. Figure 1 (a, b, c) shows the time domain original Ricker wavelet and its amplitude and phase spectrum respectively. The normalized logarithmic amplitude spectrum and the original phase spectrum are shown in Figure 1 (e, f). The inverse Fourier transform of the modified amplitude and the original phase spectra was calculated to gain the improved resolution seismic trace

which is shown in Figure 1 (d). Comparing Figures 1 (a) and (d) shows that the employed algorithm can improve the temporal resolution of seismic trace. Since the amplitude spectrum can be changed in the above mentioned process, the obtained wavelet cannot be classified in Ricker wavelet family. However, the high resolution wavelet is also close to the Ricker wavelet and increasing the resolution of the data is more important than this.

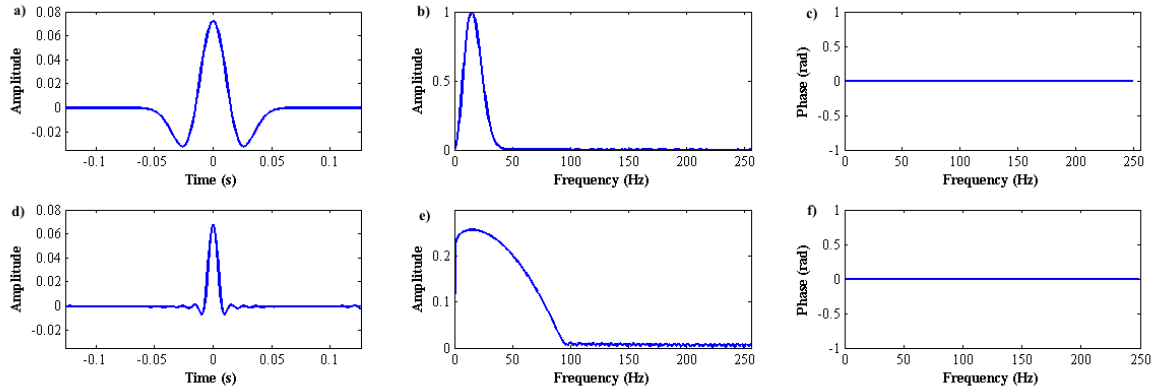

Figure 1
(a) Input wavelet: 15 Hz Ricker wavelet in time domain and its (b) amplitude and (c) phase spectrum. (d) Reconstructed high resolution wavelet from (e, f) the normalized logarithmic amplitude spectrum and the original phase spectrum of input wavelet.

Because of the Fourier transform limitations in analyzing non-stationary signals such as seismic trace, the Fourier transform was replaced with time-frequency transform in the above mentioned algorithm. There are various types of time-frequency transforms (Boashash, 2003), but the short time Fourier transform (STFT) is used herein which is the usual and common time-frequency transform (Gabor, 1946). The STFT of a time domain signal, $x(t)$, can be calculated as follows:

$$X(t,f)=\int_{-\infty}^{+\infty} x(\tau)\,g(\tau-t)\,e^{-i2\pi f\tau}\,d\tau \tag{3}$$

where, $g(t)$ is a Gaussian window and $X(t,f)$ is the time-frequency representation of time domain signal. In general, the $X(t,f)$ is a complex value and can be represented by amplitude and phase as reads:

$$\begin{aligned} A(t,f) &= \sqrt{[\mathrm{real}(X(t,f))]^2+[\mathrm{imag}(X(t,f))]^2} \\ \Phi(t,f) &= \tan^{-1}\left(\frac{\mathrm{imag}(X(t,f))}{\mathrm{real}(X(t,f))}\right) \end{aligned} \tag{4}$$

where, $A(t,f)$ and $\Phi(t,f)$ are the amplitude and phase spectrum of the time-frequency representation of time domain signal. The time domain Ricker wavelet and its amplitude spectrum of both Fourier and STFT transforms are shown in Figure 2. To calculate the time-frequency representation, the Gaussian window with a length equal to one quarter of the signal length is used. The Gaussian window is shifted by one sample along the time axis.

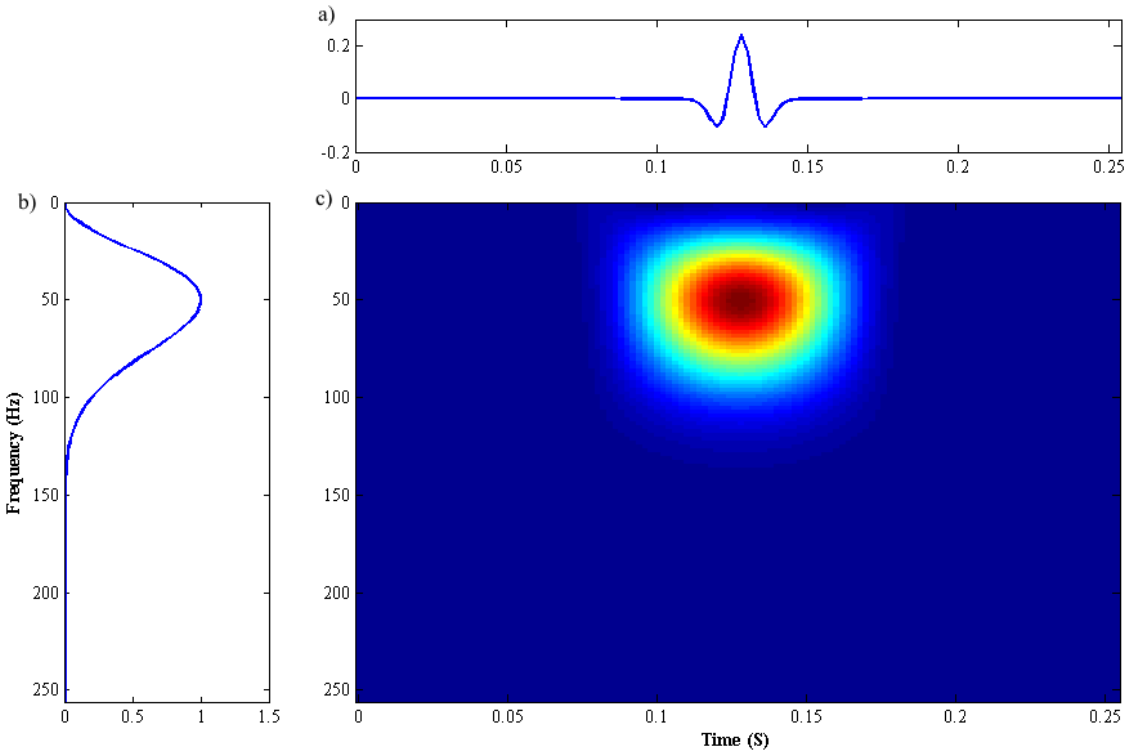

Figure 2
(a) 40 Hz Ricker wavelet in time domain, (b) its spectrum of Fourier transform, and (c) short time Fourier transform.

The method of seismic resolution improving based on cepstrum in STFT domain also consists of three steps (Sajid and Ghosh, 2014). In the first step, the trace spectrogram is calculated through the STFT by using the Gaussian window as described in Equation 3. The second step is the calculation of the logarithmic amplitude of the trace spectrogram as given below:

$$LF(t,f)=\ln\left(A(t,f)\right) \tag{5}$$

Similar to the method based on Fourier transform, the logarithmic amplitude spectrum is made purely positive by subtracting its minimum value from all the spectral values. In the final step, the normalized logarithmic amplitude of the trace spectrogram is calculated by Equations 6 and 7:

$$LFP(t,f)=LF(t,f)-\min\left(LF(t,f)\right) \tag{6}$$

$$LFPE(t,f)=LFP(t,f)\times\left(\frac{\int A(t,f)\,df}{\int LFP(t,f)\,df}\right) \tag{7}$$

Now, one can obtain the high resolution seismic trace by using the modified amplitude spectrum and the original phase spectrum as described in Equations 8 and 9:

$$\hat{X}(t,f) = LFPE(t,f) \times \exp\left(j\Phi(t,f)\right) \tag{8}$$

$$\hat{x}(t) = \int_{-\infty}^{+\infty}\int_{-\infty}^{+\infty} \hat{X}(\tau,f)\, g(t-\tau) e^{i2\pi ft} df d\tau \tag{9}$$

The flowchart of the abovementioned method is shown in Figure 3. The method of seismic resolution improving based on cepstrum in STFT domain was tested on 40 Hz Ricker wavelet. In Figure 4, the 40 Hz Ricker wavelet before and after the application of the algorithm and their STFT spectrogram are displayed. As can be seen, the employed algorithm compacted the wavelet in time domain while extended it in frequency domain without generating false features.

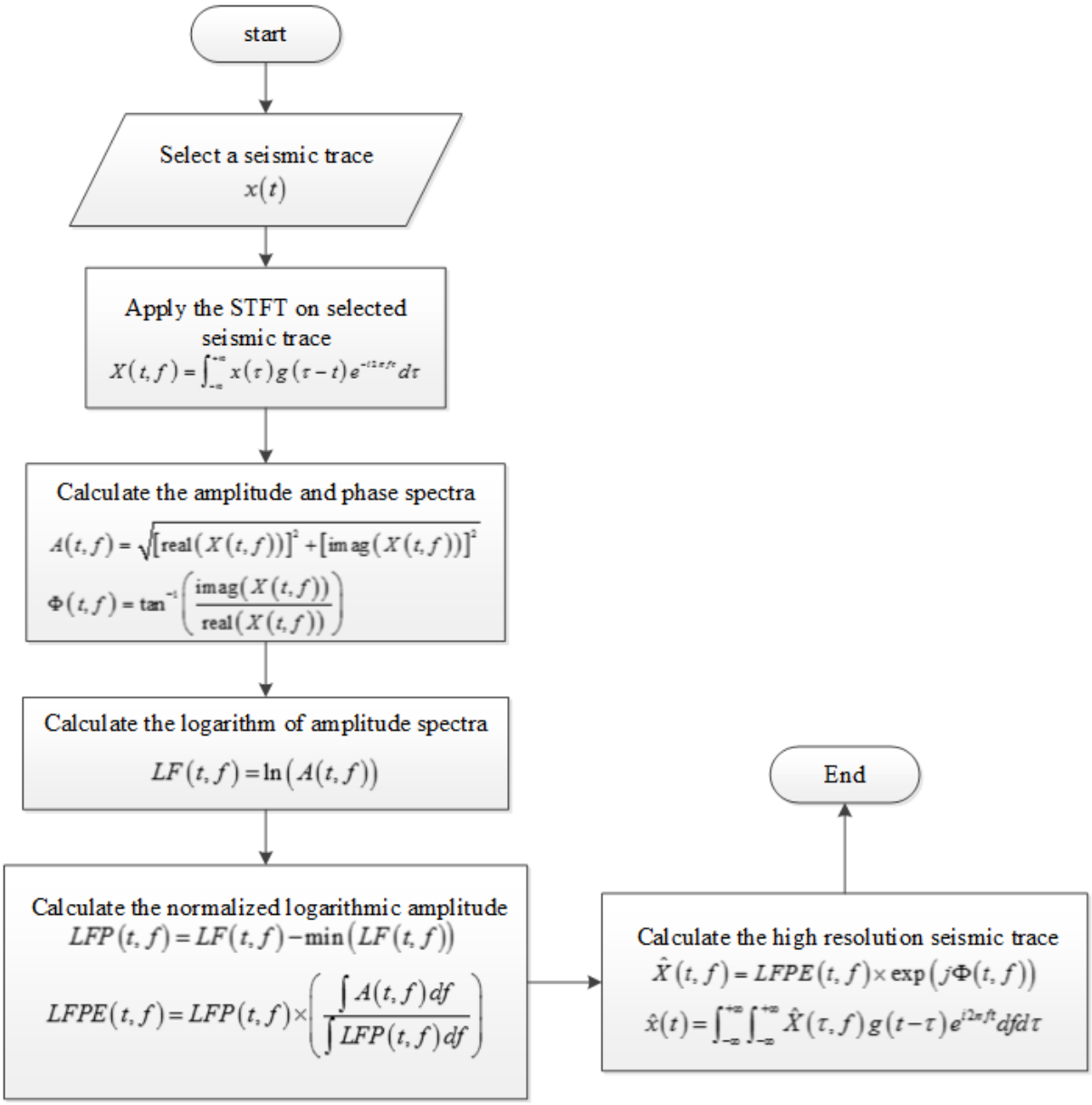

Figure 3
Flowchart of the logarithmic time-frequency transform method for the improvement in seismic temporal resolution.

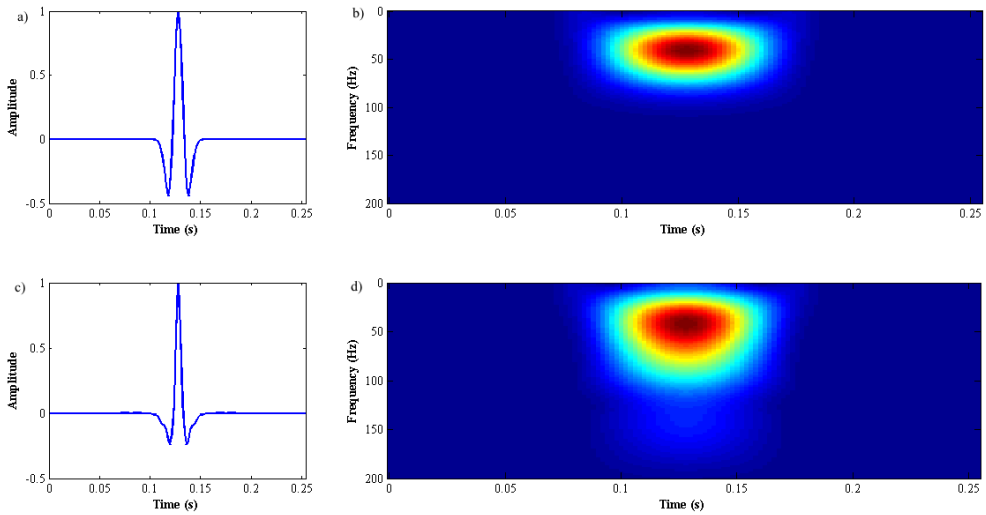

Figure 4
(a) Input wavelet: 40 Hz Ricker wavelet in time domain, (b) its STFT spectrogram; (c) reconstructed wavelet and (d) its STFT spectrogram.

The results of the mentioned algorithm are affected by the length of the frequency smoothing window in time-frequency representation calculation. Figure 5 shows the results of the employed algorithm for various lengths of frequency smoothing window. As can be seen, increasing the window length enhances the temporal resolution; the high-frequency side lobes also increase. Thus the selection of the appropriate window is a trade-off problem and one may conclude that the window length equal to one-fourth the length of the signal is the best choice.

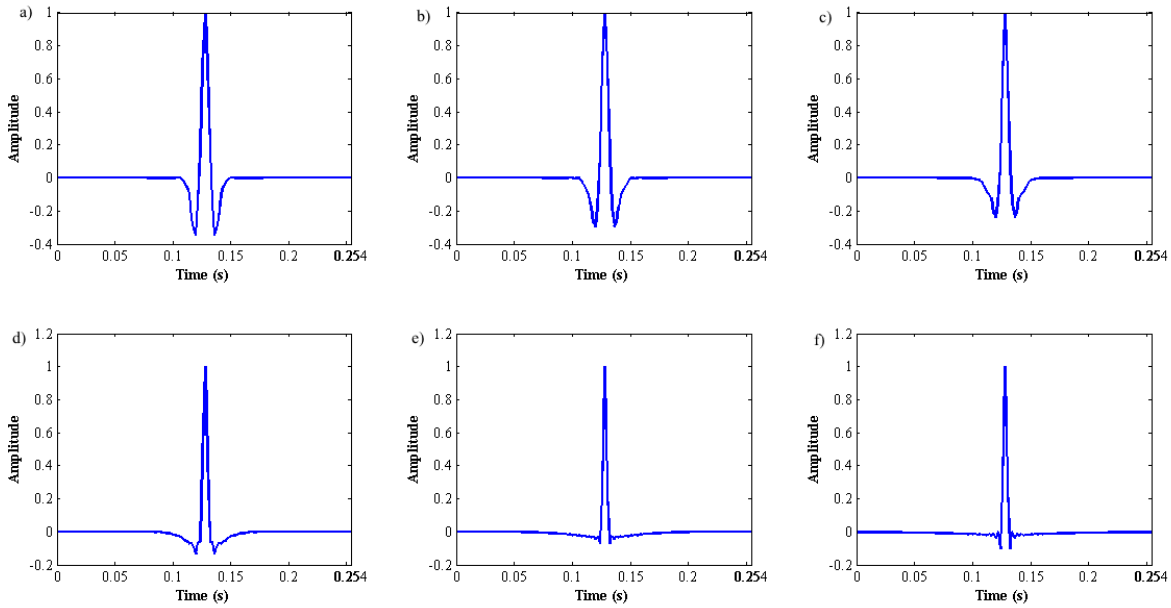

Figure 5
Reconstructed high resolution wavelet with the length of frequency window equal to (a) one-tenth of signal length, (b) eighth of signal length, (c) sixth of signal length, (d) a quarter of signal length, (e) half of signal length, and (f) signal length.

3. Results and discussion

3.1. Synthetic data

To investigate the efficiency of the abovementioned algorithm, the employed method was applied to a synthetic 2D seismic section. The geological model used to generate the synthetic 2D seismic section is shown in Figure 6. Figures 7a and 7b show the free-noise synthetic seismic section and its average amplitude spectrum respectively. The synthetic data consist of a single reflector, a thin layer, and a wedge-shape model. Due to the low temporal resolution in original synthetic seismic section, it is not possible to separate the reflections from the top and bottom of the thin layer. Moreover, the reflections from the top and bottom of the edge are detectable at trace 25.

The result of applying the method to the synthetic seismic section is shown in Figure 7c. As can be seen, the temporal resolution of seismic section is dramatically increased. The reflections from the top and bottom of thin layer are fully recognizable. It can be observed in the wedge model that the reflections, which were started to full interference at trace 25, were still separable up to trace 39. The average amplitude spectrum of the output seismic section is shown in Figure 7d. To compare the results more accurately, the amplitude spectrums of two seismic traces (No. 10 and 31) before and after the seismic resolution enhancement are displayed in Figures 7e and 7f.

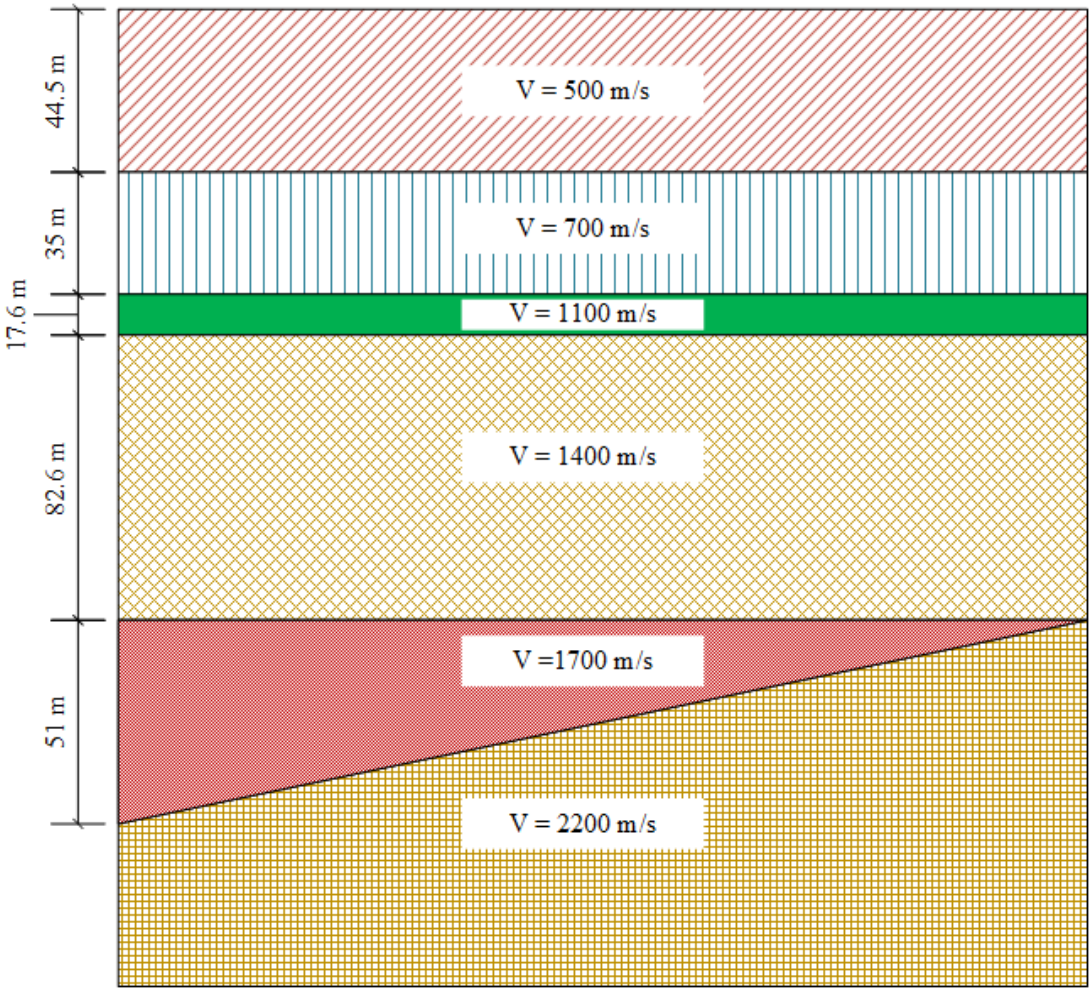

Figure 6
Synthetic geologic model to generate the synthetic seismic data.

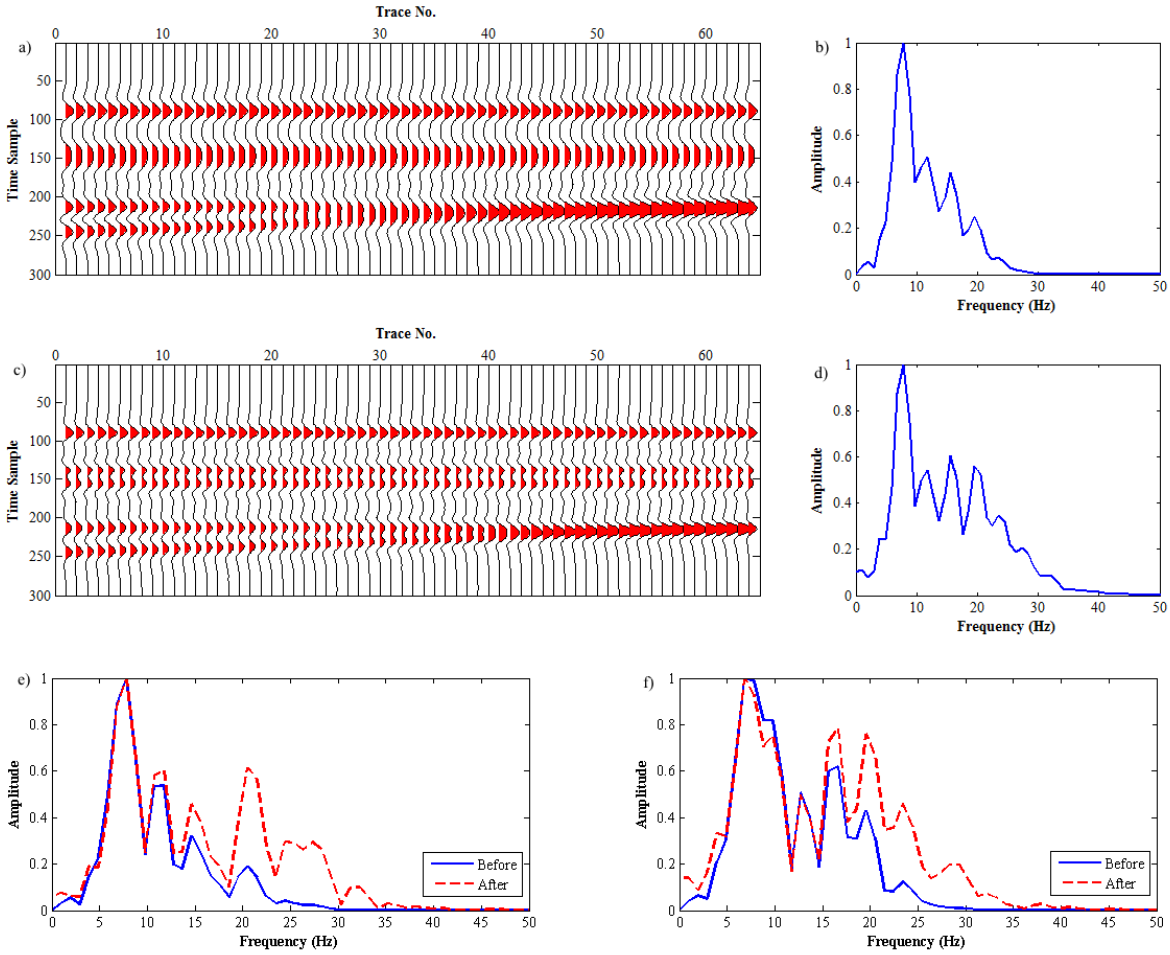

Figure 7

(a) Free-noise synthetic seismic section and (b) its average amplitude spectrum; (c) synthetic seismic section after the application of the propose method and (d) its average amplitude spectrum; (e) and (f) the amplitude spectrum of 31st and 10th traces before (blue line) and after (red dashed line) resolution enhancement.

To evaluate the performance of the method in the presence of noise, the white Gaussian noise was added to the synthetic seismic section (signal to noise ratio equal to 21 dB) and the method was applied to the noisy data. According to the results shown in Figure 8, the algorithm performance is good even in the presence of noise.

We compared the obtained results of the synthetic data in both noisy and noise-free cases with the results of frequency domain deconvolution (Yilmaz and Doherty, 2001) shown in Figure 9. Frequency deconvolution is performed by free MATLAB toolbox entitled CREWES. As can be seen in Figure 9a, the performance of the two techniques is very similar in the noise free synthetic data case. However, it can be realized that the frequency domain deconvolution has created some noise in the output. The mentioned disadvantage becomes more visible in noisy data (Figure 9b).

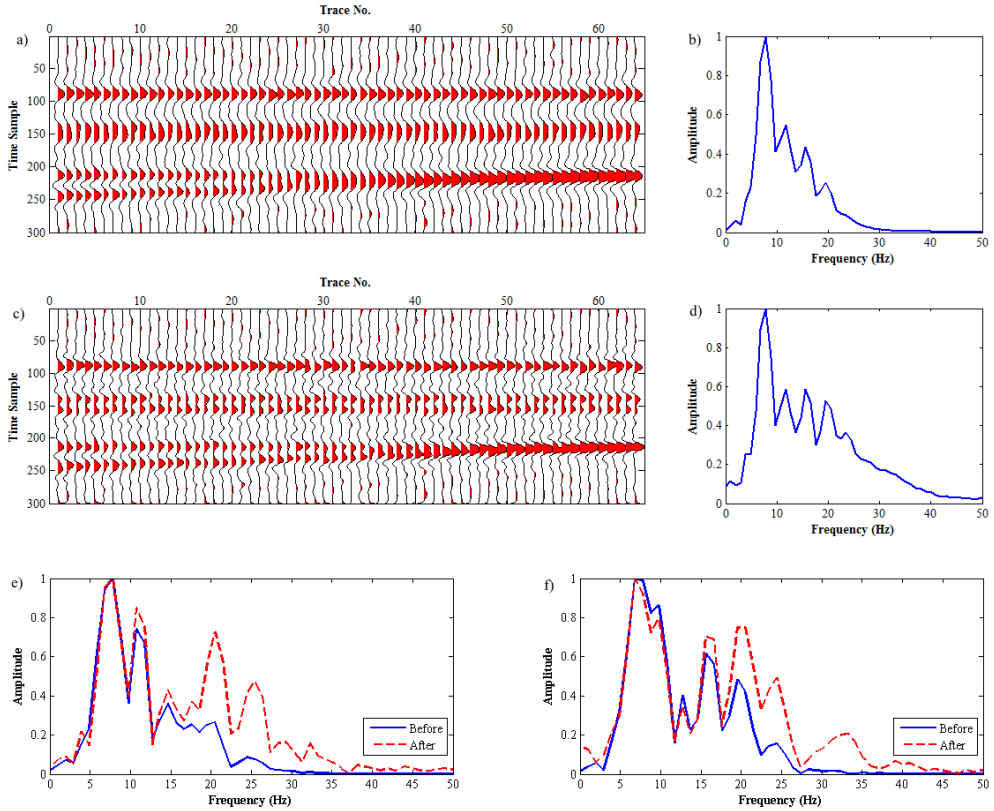

Figure 8

(a) Noisy synthetic seismic section and (b) its average amplitude spectrum; (c) noisy synthetic seismic section after the application of the propose method and (d) its average amplitude spectrum; (e) and (f) the amplitude spectrum of 31st and 10th traces before (blue line) and after (red dashed line) resolution enhancement.

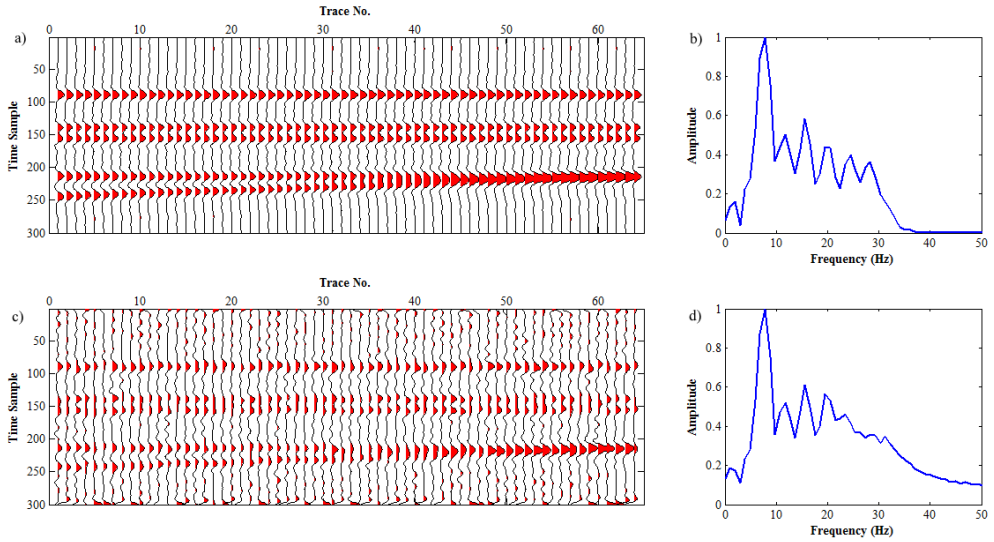

Figure 9

(a) Free noise synthetic seismic section (Figure 7a) after the application of the frequency domain deconvolution and (b) its average amplitude spectrum; (c) noisy synthetic seismic section (Figure 8a) after the application of the frequency domain deconvolution and (d) its average amplitude spectrum.

The sensitivity to noise of the seismic resolution improving method based on cepstrum in STFT domain was investigated by varying the level of the signal to noise ratio in the synthetic data. Figure 10 shows the results of the method for synthetic seismic data with four levels of noise, namely 18, 14, 12.5, and 9.5 dB. It can be seen that the results are almost acceptable as long as the signal to noise ratio is 14 dB.

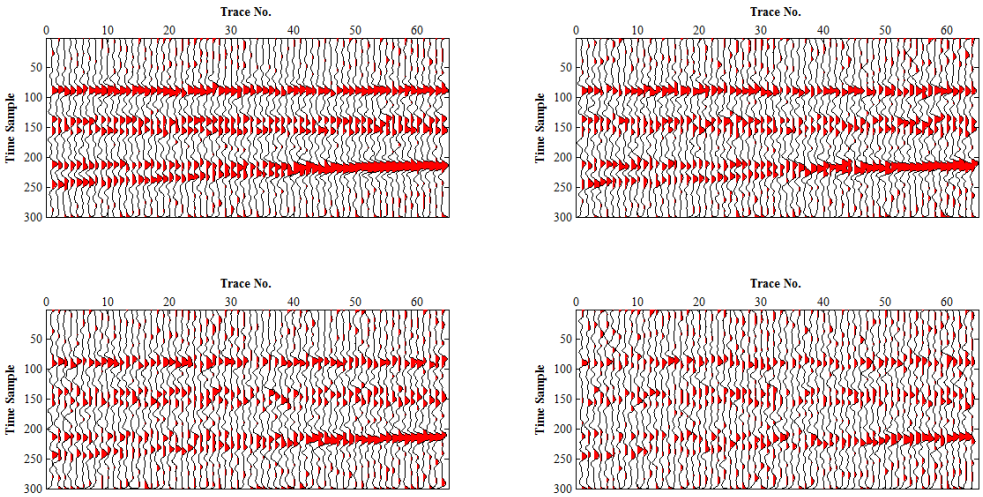

Figure 10
Results of applying the employed method for noisy synthetic data with different values of the signal to noise ratio: (a) 18 dB, (b) 14 dB, (c) 12.5 dB, and (d) 9.5 dB.

3.2. Field data

In addition, the method was applied to a field seismic data from one of hydrocarbon fields in the southwest of Iran. The real seismic sections before and after the application of method are shown in Figures 11a and 11b. The time-frequency representation of real seismic data before and after the application of the proposed algorithm is shown in Figures 11d and 11e. It can be seen that the frequency bandwidth of the seismic data is expanded during applying the proposed algorithm. Moreover, the obtained results of the real data were compared with the results of frequency domain deconvolution shown in Figure 11c. It is clear that the presence of high frequency noise in the deconvolved section reduces the quality of data. It can be easily observed that the resolution of the real seismic data is considerably increased and many hidden features are discovered. For a closer look, three windows of the data before and after applying the algorithm were chosen and magnified in Figure 12. When comparing their amplitude spectra as shown in Figure 13, it can be seen that the field seismic data after applying the algorithm have a broader amplitude spectrum than the original real data.

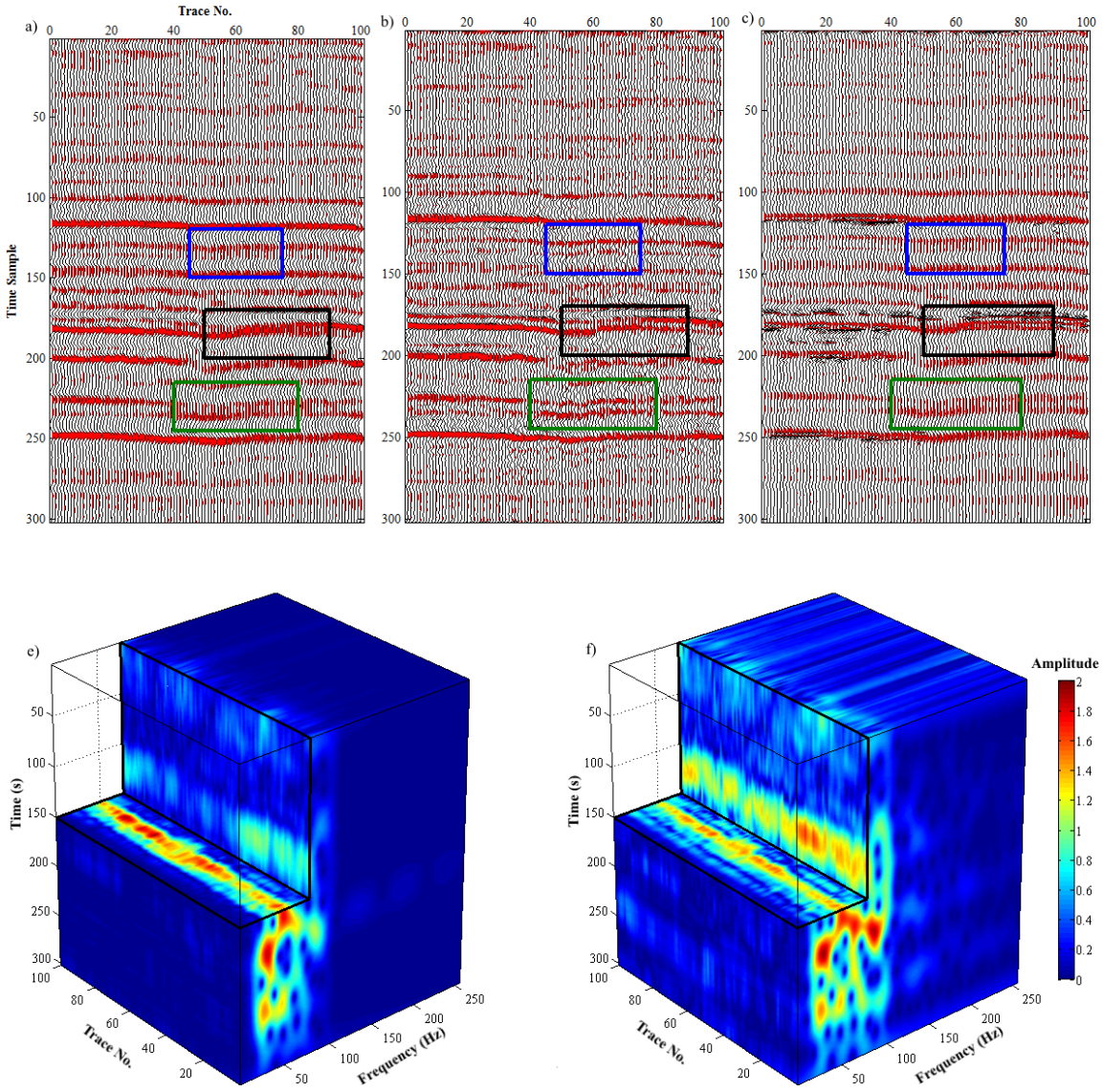

Figure 11

Real seismic data (a) before and (b) after the application of the proposed algorithm; (c) real seismic data after the application of the frequency domain deconvolution; the time-frequency representation of real seismic data (d) before and (e) after the application of the proposed algorithm.

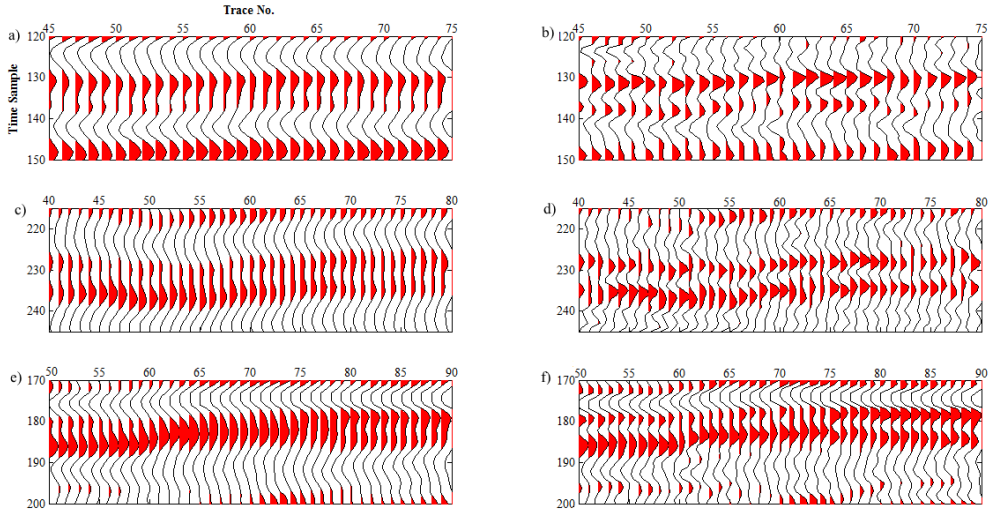

Figure 12
(a, b) The blue window in Figure 11 before and after the application of the proposed algorithm respectively; (c, d) the green window in Figure 11 before and after the application of the proposed algorithm respectively; (e, f) the black window in Figure 11 before and after the application of the proposed algorithm respectively.

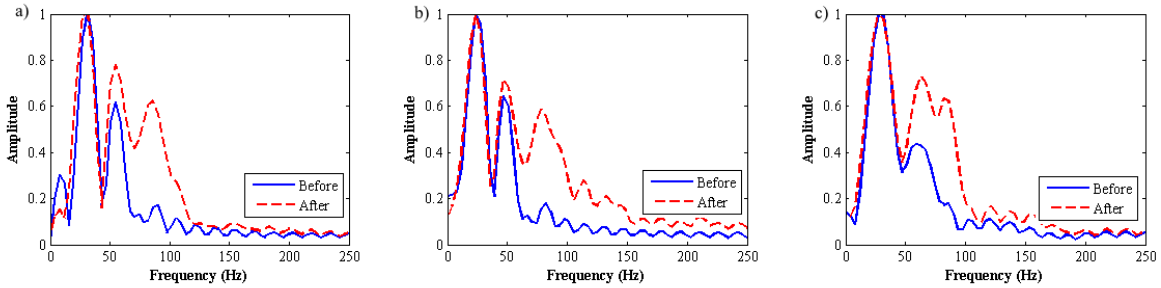

Figure 13
Average amplitude spectrum of (a) the blue window in Figure 9 before (blue line) and after (red dashed line) resolution enhancement, (b) the green window in Figure 9 before (blue line) and after (red dashed line) resolution enhancement and (c) the black window in Figure 9 before (blue line) and after (red dashed line) resolution enhancement.

4. Conclusions

A new algorithm is introduced which improves the temporal resolution of seismic data by using the logarithmic time-frequency transform method. The algorithm uses valuable properties of both the time-frequency transform and the cepstrum to extend the frequency band at each translation of the spectral decomposing window. The results of the application of the algorithm to both synthetic and real seismic data show that the introduced method can increase the temporal resolution of the seismic data. Furthermore, the results of the algorithm in the presence of noise show that the algorithm can improve the temporal resolution of the seismic data without greatly boosting noise. However, the employed method makes a little change in the wavelet shape which can be neglected.

5. Nomenclature

t	: Time
f	: Frequency
$x(t)$	: Seismic trace in time domain
$X(f)$	: Seismic trace in frequency domain
$A(f)$	: Amplitude spectrum of seismic trace
$\Phi(f)$	: Phase spectrum of seismic trace
$X(t, f)$	: Time-frequency transform of seismic trace
$g(t)$	: Gaussian window for time-frequency transform computing
$A(t, f)$	: Amplitude spectrum of time-frequency transform of seismic trace
$\Phi(t, f)$	: Phase spectrum of time-frequency transform of seismic trace
$LF(t, f)$	: Logarithm of amplitude spectrum of time-frequency transform of seismic trace
$LFP(t, f)$	: $LF(t, f)$ which is made purely positive
$LFPE(t, f)$	: $LFPE(t, f)$ which is normalized
$\hat{X}(t, f)$	: Modified time-frequency transform of seismic trace
$\hat{x}(t)$	: Estimated high resolution seismic trace

References

Badley, M. E., Practical Seismic Interpretation, International Human Resources Development Corporation, the University of Michigan, 266 p.1985.

Boashash, B., Time Frequency Analysis, Elsevier Science, 770 p. 2003.

Gabor, D., Theory of Communication, Part 1: The Analysis of Information, Journal of the Institution of Electrical Engineers - Part III: Radio and Communication Engineering, Vol. 93, No. 26, p. 429-441, 1946.

Herrera, R. H. and Van der Baan, M., Short-time Homomorphic Wavelet Estimation, Journal of Geophysics and Engineering, Vol. 9, No. 6, p. 674-680, 2012.

Matos, M. C. d. and Marfurt, K., Complex Wavelet Transform Spectral Broadening, SEG Technical Program Expanded Abstracts, p. 1465-1469, 2014.

Oppenheim, A. V., Willsky, A. S., and Nawab, S. H., Signals and Systems, Prentice Hall, 957 p. 1997.

Proakis, J. G. and Manolakis, D. G., Digital Signal Processing, Principles, Algorithms, and Applications, Pearson Prentice Hall, 948 p., 2007.

Sajid, M. and Ghosh, D., Logarithm of Short-time Fourier Transform for Extending the Seismic Bandwidth, Geophysical Prospecting, Vol. 62, No. 5, p. 1100–1110, 2014.

Shang, B. Z. and Caldwell, D. H., A Bandwidth Enhancement Workflow through Wavelet Analysis, SEG Technical Program Expanded Abstracts, p. 2012-2015, 2003.

Sheriff, R. E. and Geldart, L. P., Exploration Seismology, Cambridge University Press, 2nd Edition, 1995.

Wang, Y., Seismic Inverse Q Filtering, Wiley-Blackwell, 248 p., 2008.

Yilmaz, Ö. and Doherty, S. M., Seismic Data Analysis: Processing, Inversion, and Interpretation of Seismic Data, Society of Exploration Geophysicists, 2001.

Zhou, H., Wang, C., Marfurt, K. J., Jiang, Y., and Bi, J., Enhancing the Resolution of Seismic Data Using Improved Time-frequency Spectral Modeling, SEG Technical Program Expanded Abstracts, p. 2656-2661, 2014.